

3. Realization of the U.S. national scale of radiance temperature

3.1 1990 NIST scale of radiance temperature

The reference temperature standard, a gold fixed-point blackbody (Au) with a temperature (T_{Au}) of 1064.18 EC (1337.33 K), and the Planck radiation law are used to realize and disseminate the 1990 NIST Radiance Temperature Scale. Equation (5) is used to calculate the spectral radiance $L_{\mathcal{S}Au}(\mathcal{S} T_{Au})$ of the fixed-point blackbody for $\mathcal{S}= 655.3$ nm in all the measurements of this calibration facility. Measurements are performed from 800 °C to 2300 °C for lamps, from 800 °C to 2700 °C for radiation thermometers, and extrapolated to 4200 °C for some disappearing filament optical pyrometers.

The NIST PEP is the transfer device used to compare the spectral radiances of the sources by the direct substitution method. The signals are corrected for size of source, amplifier gain, and linearity. With these corrections, the spectral radiance and the radiance temperature can be determined from eqs (12) and (13). The NIST PEP is a filtered radiometer that uses two interference filters to select the bandpass. The spectral bandwidth is 5 nm with a mean effective wavelength of 655.3 nm. A photomultiplier tube with an S-20 spectral response is used in the dc mode. The measurement spot size is a 0.6 mm by 0.8 mm rectangle.

A high stability vacuum lamp operated at a single radiance temperature of approximately 1255 °C is the working standard (WS). By equating eqs (9) and (13), the spectral radiance ratio is

$$r_1 = \frac{L_1(T_{WS1})}{L_1(T_{Au})} = \frac{S_{WS1}}{S_{Au}}. \quad (15)$$

After applying correction factors to the signals in eq (15) for amplifier calibration (C_A), linearity (C_L), and size of source (C_S), the spectral radiance of the WS1 lamp can be written as

$$L_{WS} = \frac{e_{Au} \cdot c_{1L}}{n_1^2 \cdot I^5 \cdot \left[\exp\left(\frac{c_2}{n_1 \cdot I \cdot T_{Au}}\right) - 1 \right]} \cdot r_1 \cdot \frac{(C_A \cdot C_L \cdot C_S \cdot G)_{WS}}{(C_A \cdot C_L \cdot C_S \cdot G)_{Au}}. \quad (16)$$

References regarding linearity issues are presented in Section 3.3.5. The uncertainty analysis in Section 3.6 can then be derived from eq (15) for the NIST radiance temperature scale up to the calibration of the spectral radiance of the working standard lamp.

3.2 Temperature standards

3.2.1 Gold-point blackbody

In the RTCL, a gold fixed-point blackbody with a calculated emissivity of 0.9999, designed and built by the NIST Optical Technology Division, is the primary standard used to realize the 1990 NIST Radiance Temperature Scale. The blackbody in figure 3 consists of a graphite cavity, a crucible of gold, and a cylindrical heat-pipe furnace. The cavity, which is

76 mm in length and 6 mm in diameter and has a 60E conical end shown, is made from Ultra “F” grade graphite (spectrographic purities of 10 ppm or less). Surrounding this cavity is a crucible containing 0.99999% pure gold. The cavity, along with graphite rings and silica glass spacers, is placed in an alumina tube. The front rings define a solid angle with a $f/6$ field of view, while the back rings support the thermocouple. A furnace (see fig. 3), which consists of a sodium heat-pipe heated by two semi-cylindrical ceramic heater elements inside of a mullite tube, is enclosed in a water-cooled housing (631 mL/min) and is operated in an argon environment (37 mL/min with furnace door closed and 235 mL/min with furnace door open).

The gold-point blackbody liquid-to-solid phase transition is shown in figure 4. The duration of a melt or freeze plateau is approximately 40 min, and the time delay between these observation periods is about 45 min. Measurements during the freeze cycle show a negative slope of 20 mK in 30 min. The blackbody is slowly heated over about 8 h before reaching the melting point and is typically ramped up over night so that it is held just below the melting point the next morning. After the initial heating at 8 A, the melt cycle is begun by increasing the current to 8.5 A until the temperature reaches 1071 EC. The freeze cycle is begun by lowering the blackbody current to 7.95 A. Then the blackbody current is raised to 8.5 A at 1050 EC to begin the melt cycle again.

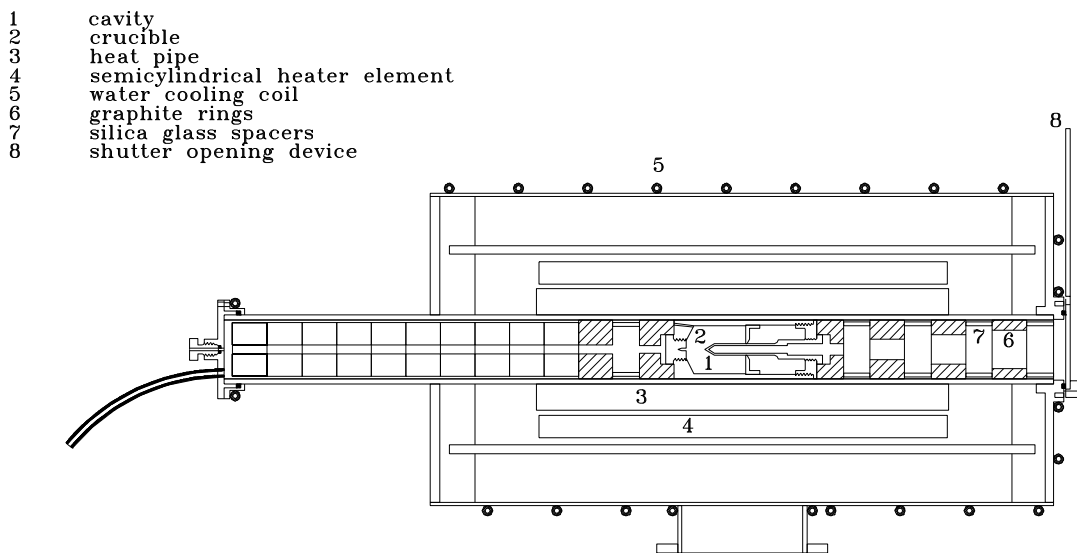


Figure 3. Schematic of gold-point blackbody.

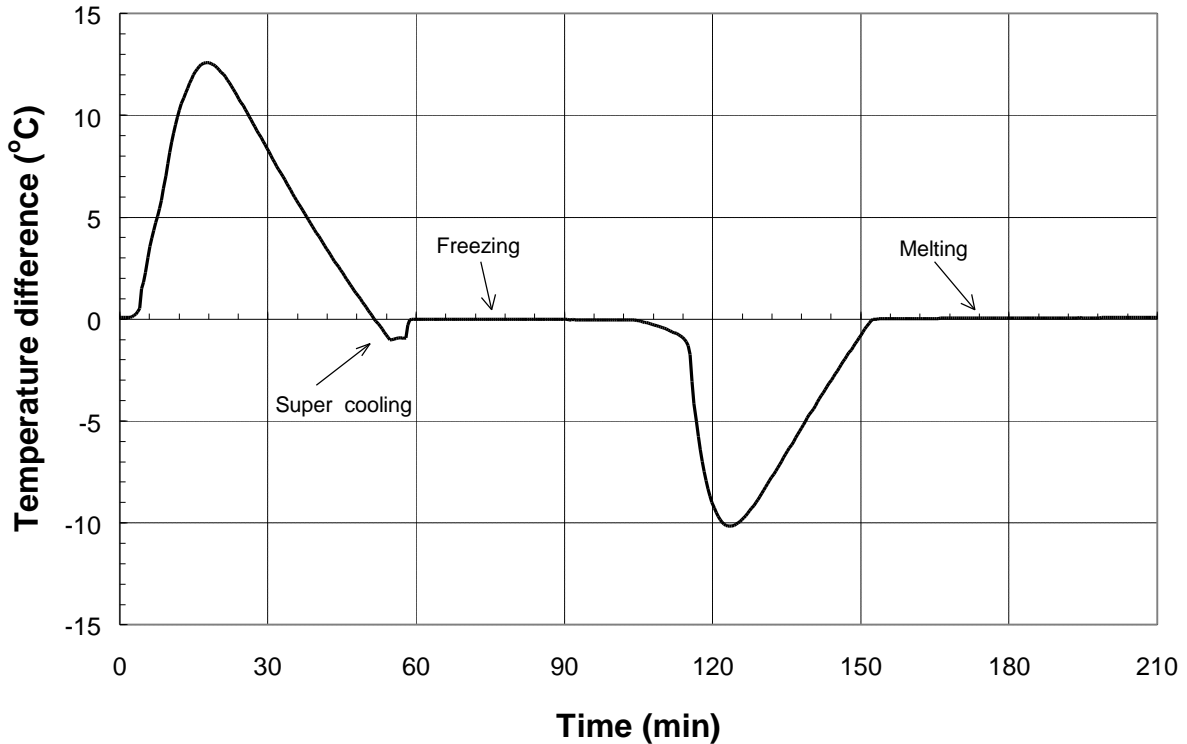
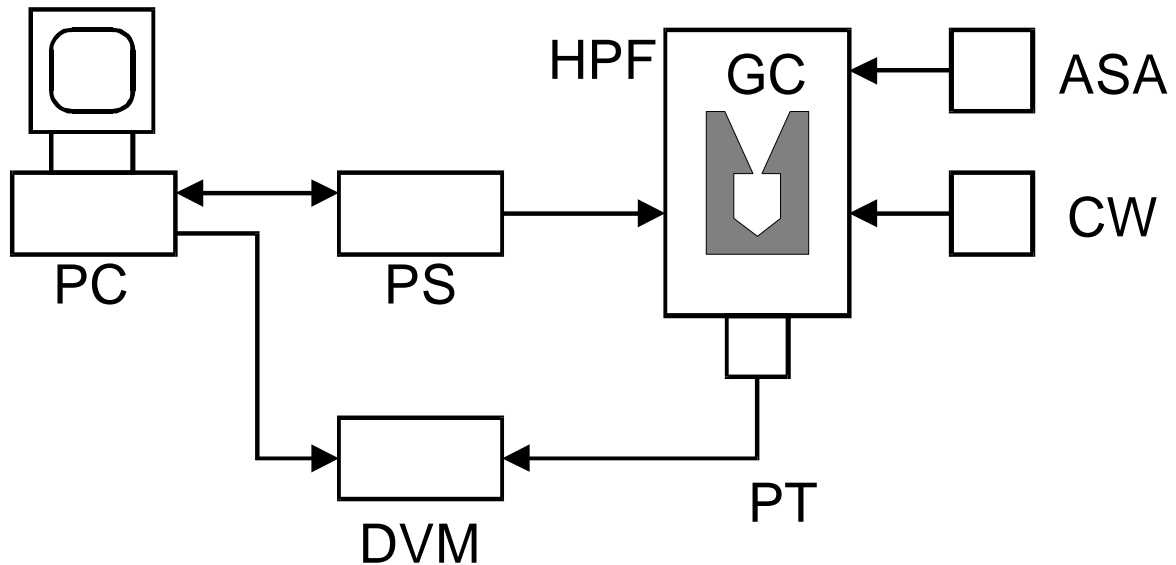


Figure 4. Gold-point blackbody liquid-to-solid phase transition.

The gold-point blackbody control system shown in figure 5 consists of a 286-based personal computer, which regulates the power supply and reads the thermocouple measurements from the digital voltmeter. To monitor the set points, platinum and platinum/10% rhodium (type S) thermocouples are inserted into round double bore alumina tubing and are placed in a silica glass sheathing which makes contact with the rear end of the crucible.

3.2.2 Tungsten ribbon filament lamps

Because of a reproducible radiance temperature versus lamp current relationship, tungsten ribbon filament lamps are used in the radiance temperature scale realization and are issued as radiance temperature standards. Vacuum lamps are typically used for temperatures from 800 °C to 1700 °C, and argon gas-filled lamps for temperatures from 1300 °C to 2300 °C. Gas is introduced into the high temperature lamps to slow down the evaporation rate of the tungsten. The evaporated tungsten atoms collide with the gas atoms, lose their energy, and re-condense on the filament surface before being swept away by convection [9].



LEGEND

ASA	Argon Supply and Alarm
CW	55 °C Chilled Water/Cold Water Switch
DVM	Digital Voltmeter
GC	Gold-filled Crucible
HPF	Heat Pipe Furnace
PC	Personal Computer
PS	Power Supply
PT	Pt/Pt-10% Rh Thermocouple (Type S)

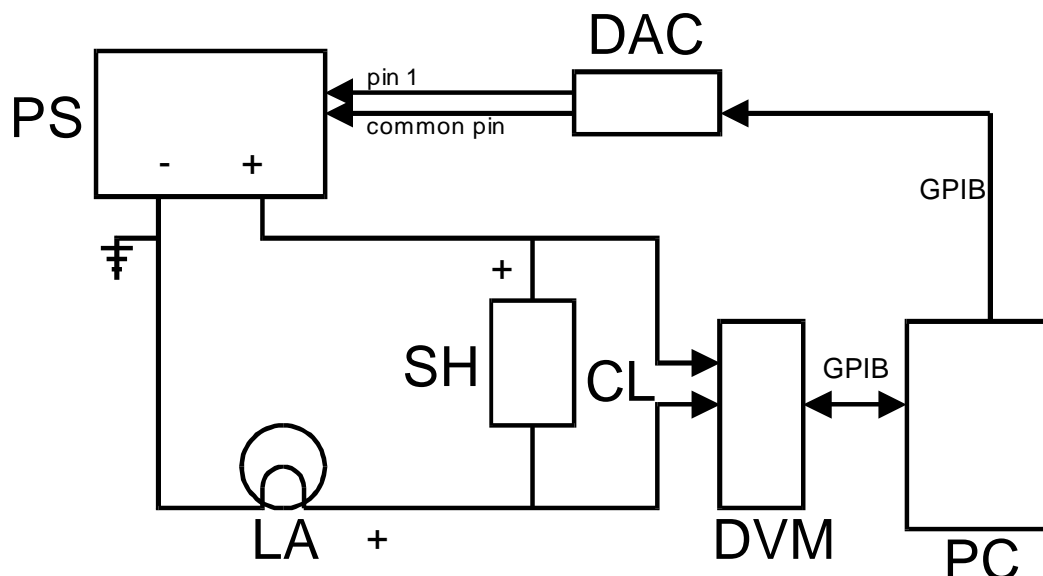
Figure 5. Gold-point blackbody control system.

The lamps have cylindrical glass envelopes and are operated on direct current with the base facing downward. A computer-stabilized power supply regulates the lamp current to within ± 0.2 mA. A schematic of the lamp current monitoring system is shown in figure 6. The filament is connected to the screw base by wires, which conduct the current and thereby minimize contact problems associated with the screw bases. To achieve the required precise alignment, the lamps are rigidly fastened in source mounts that allow translation along and rotation about three mutually perpendicular axes. Located at the intersection of the center of the lamp filament at the height of the notch opening, the rectangular calibration area on the surface of the lamp filament is 0.6 mm wide by 0.8 mm high. The notch is about midway along one edge of the filament. An alignment mark or an etched arrow is placed on the envelope opposite the side viewed by the pyrometer to permit reproducible angular positioning. Then the lamp is rotated so that the arrowhead is centered at the mouth of the notch.

Some lamps use a pointer that is connected to the filament support to indicate the calibration area. The advantage to this approach is a more uniform filament. However, one

disadvantage is the requirement of predictable filament expansion and contraction for reproducible calibration area indication by the pointer.

Until 1995, the NIST issued General Electric³ type 30A/6V/T24 ribbon filament lamps as radiance temperature standards. However, General Electric stopped manufacturing these lamps in 1990. The lamp had a glass cylindrical envelope that was 300 mm long and 75 mm in diameter and a filament that was 3 mm wide and 50 mm long. Figure 7 shows typical lamp currents as a function of temperature for the General Electric ribbon filament lamps.



LEGEND

CL	Current Sensing Leads
DAC	Two-channel 12-bit D/A Converter
DVM	Digital Voltmeter
GPIB	GPIB IEEE-488 Interface
LA	Lamp
PC	Personal Computer
PS	Power Supply
SH	0.1 Ω Shunt

Figure 6. Schematic of lamp current monitoring system.

³ Certain commercial equipment, instruments, or materials are identified in this paper for the sole purpose of adequately describing experimental or test procedures. Such identification does not imply recommendation or endorsement by the National Institute of Standards and Technology of a particular product, nor does it imply that the materials or equipment identified are necessarily the best available for the purpose it serves.

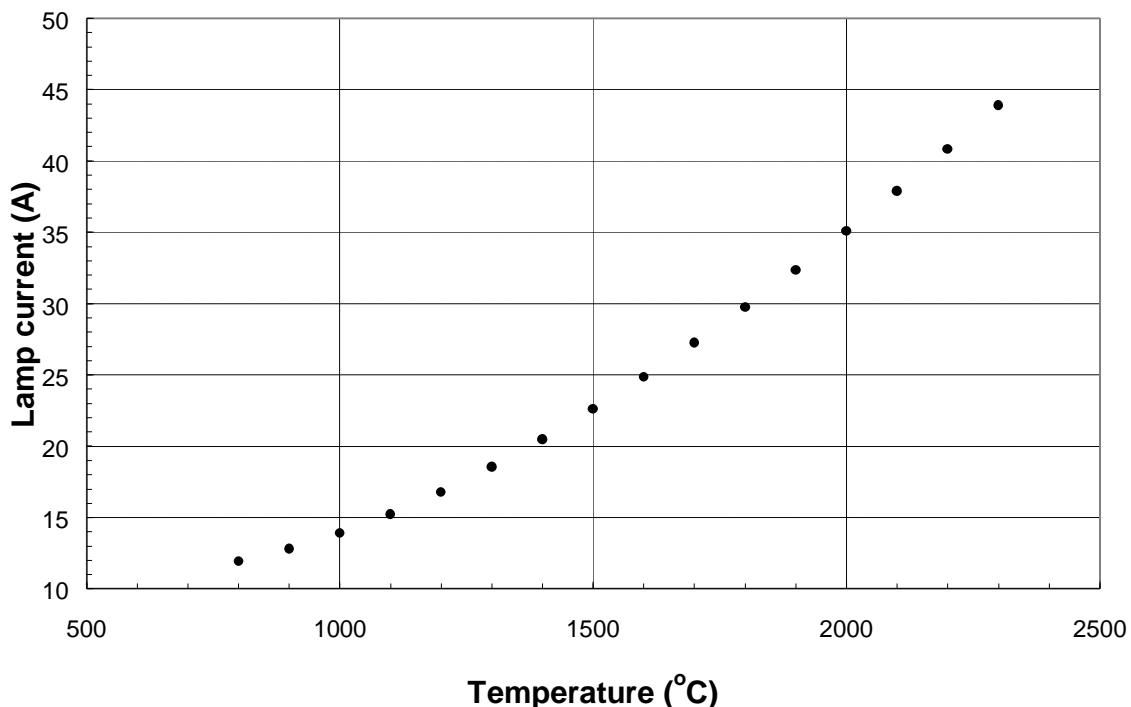


Figure 7. Typical lamp currents for the General Electric 30A/T24/6 ribbon filament lamp.

The NIST is currently issuing U.K. General Electric Company (GEC) lamps, although the lamps are no longer available from this source. The GEC lamps (type 20/G and 20/V) have glass cylindrical envelopes that are 235 mm long with a 64 mm diameter. The 20/V is a vacuum lamp with a filament 1 mm wide by 50 mm long and requires about 10 A dc at 1500 °C. The 20/G is a gas-filled lamp with a 2 mm wide by 30 mm long filament and requires about 20 A dc at 2300 °C.

In 1992, Type TRU 1100-2350 lamps were purchased from the Moscow Lamp Factory (Russia) for testing as radiance temperature standards. Due to a decline in requests for radiance temperature standard lamps, the testing was not done. At 2300 °C, about 25 A dc current is required from the gas-filled lamp, which has a cylindrical envelope, a 2.5 mm wide by 20 mm long filament, and an alignment pointer. The TRU lamps, which have a 35 mm silica glass window that projects about 5 mm from the envelope, were used in addition to the GE lamp in the NIST/VNIOFFI spectral radiance intercomparison [10].

The NIST has also bought type 24/G lamps with double silica glass windows from Polaron Engineering LTD (U. K.) for use as working and check standards. These lamps are similar in design and construction to the GEC lamps.

3.2.3 Working standard lamps

A vacuum tungsten ribbon filament lamp of the Quinn-Lee type [11,12] is used in the temperature scale realization as the secondary temperature standard which maintains the temperature scale between scale realizations and as the transfer standard for calibration

measurements. The temperature of the working standard lamp (serial number SL20) is determined by spectral comparison with the gold-point blackbody. A drawing of this lamp is shown in figure 8. This lamp is operated at a single current (7.7788 A dc) to produce a spectral radiance about eight times higher than that of the gold-point blackbody at 655.3 nm (a radiance temperature of about 1530 K). This lamp is stable to better than 0.1 °C over 100 h when operated under these single-level conditions. A graph of the calibration history of the working standard from August 1989 to February 1996 is shown in figure 9.

3.2.4 Variable-temperature blackbody

The NIST uses a commercial variable-temperature blackbody (VTBB) for its radiance temperature transfer standard (See fig. 10). This VTBB was manufactured by Thermogage Inc. in Frostburg, MD and was supplied with the Type II dual blackbody assembly (2.54 cm or 1 in ID cavity), the 48 kW power supply, a control program, the model 7000-1 (4 range) optical pyrometer, and a digital temperature computer control module. Modifications requested by the NIST include the addition of the water-cooled semi-cylindrical mirrors, and enlarging the extension tube opening to accommodate measurements with the NIST PEP.

The VTBB is operated between 700 °C and 2700 °C. The ranges, which are selected by placing different size apertures on the optical control pyrometer, are the low range (700 °C to 1300 °C), the medium range (1300 °C to 1800 °C), the high range (1800 °C to 2500 °C), and the extra high range (2500 °C to 2700 °C). The electrodes are water-cooled by using a 13 °C (55 °F) chilled water source. Before the blackbody is turned on, argon gas displaces the air in the cavity. When the VTBB cavity is operating, the argon exits from both the front and back extension tubes.

The variable-temperature blackbody control system regulates the blackbody temperature to within ± 0.1 °C (see fig. 11). The NIST measures the uniformity of the center partition of the Thermogage heater elements, and uses those with a spatial uniformity of better than ± 0.2 °C at 2000 °C over an area of 10 mm diameter (see fig. 12). The blackbody heats up to the operating point in less than 30 min and responds quickly to temperature changes (see fig. 13). The day-to-day stability of the blackbody is better than ± 0.3 °C, and the 6-month stability is within ± 2 °C.

The VTBB operates between 800 °C and 2700 °C with an estimated emissivity of 0.99 from analytical modeling. The temperature distribution within the VTBB cavity is less than 50 °C. The blackbody cavity is composed of a single piece of graphite, which is specially tapered for achieving high temperature uniformity. This graphite tube is cylindrically hollow on both ends to form two 2.54 cm diameter cavities with a common partition in the center. One cavity is used for temperature control, and the other cavity is the blackbody source.

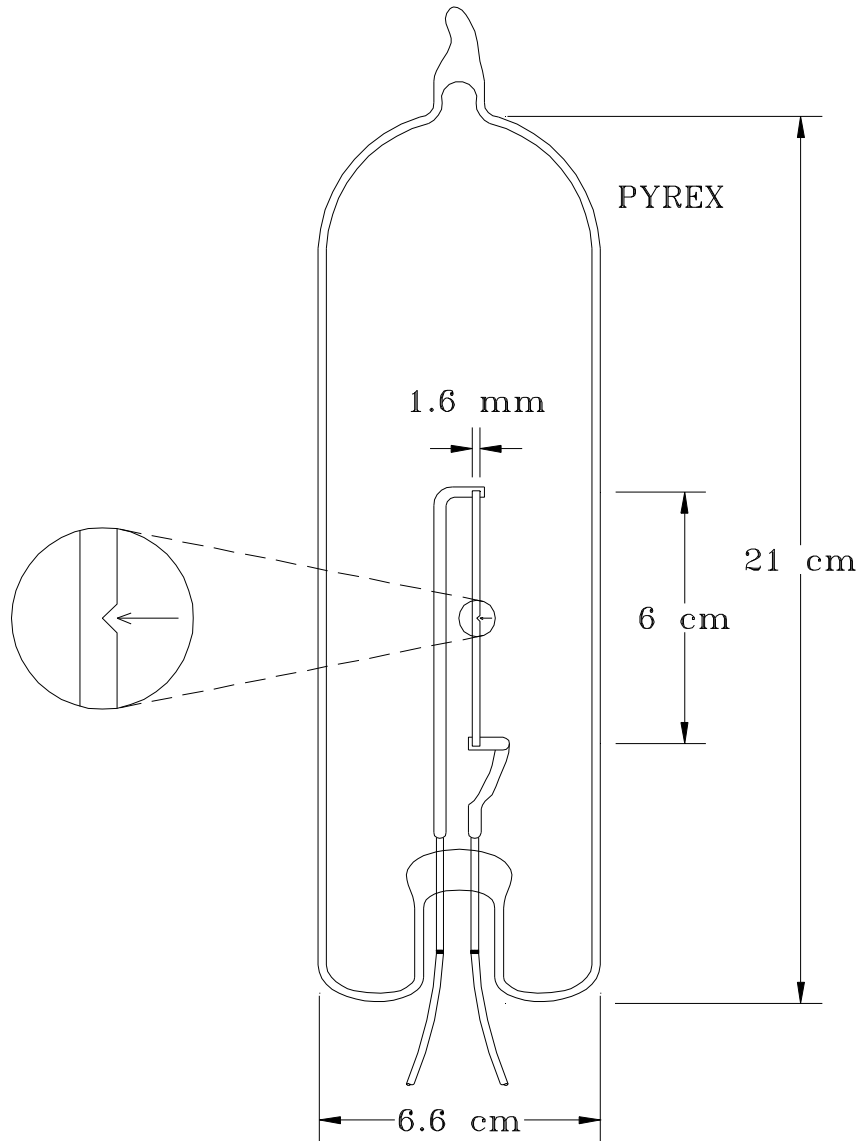


Figure 8. Ribbon filament lamp.

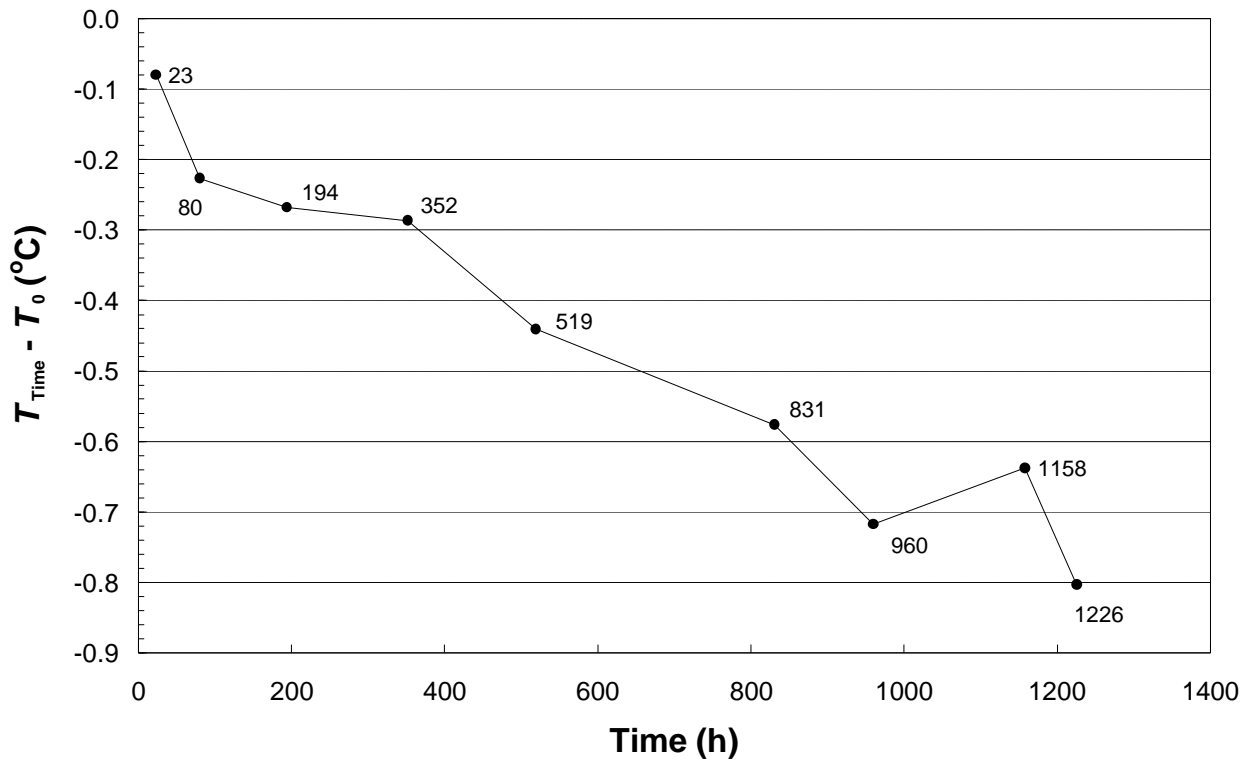


Figure 9. Calibration history of the WS (no.SL20).

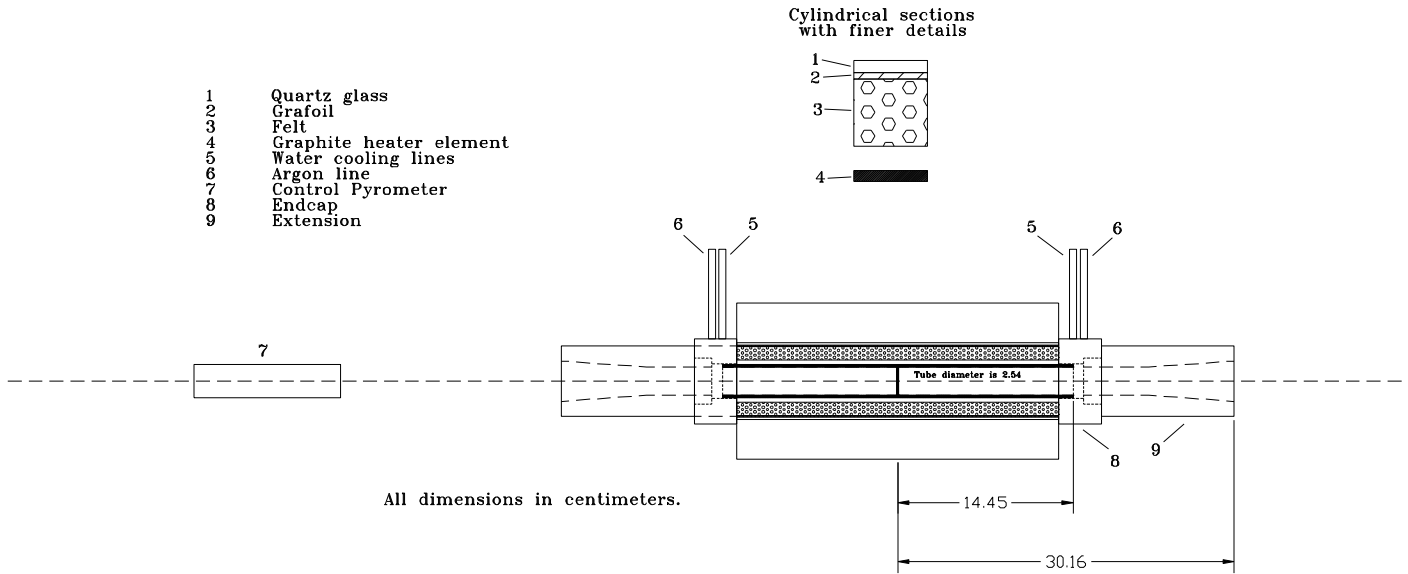
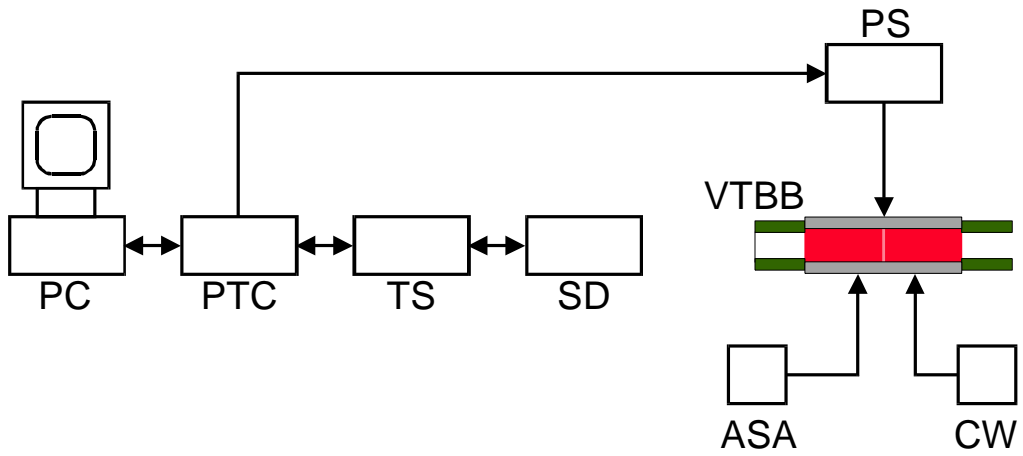


Figure 10. Schematic of variable-temperature blackbody.



LEGEND

ASA	Argon Supply and Alarm
CW	55 °C Chilled Water/Cold Water Switch
PC	Personal Computer
PS	Power Supply
PTC	PID Temperature Controller
SD	Silicon Detector
TS	Thermal Stabilizer
VTBB	Variable Temperature Blackbody

Figure 11. Variable-temperature blackbody control system.

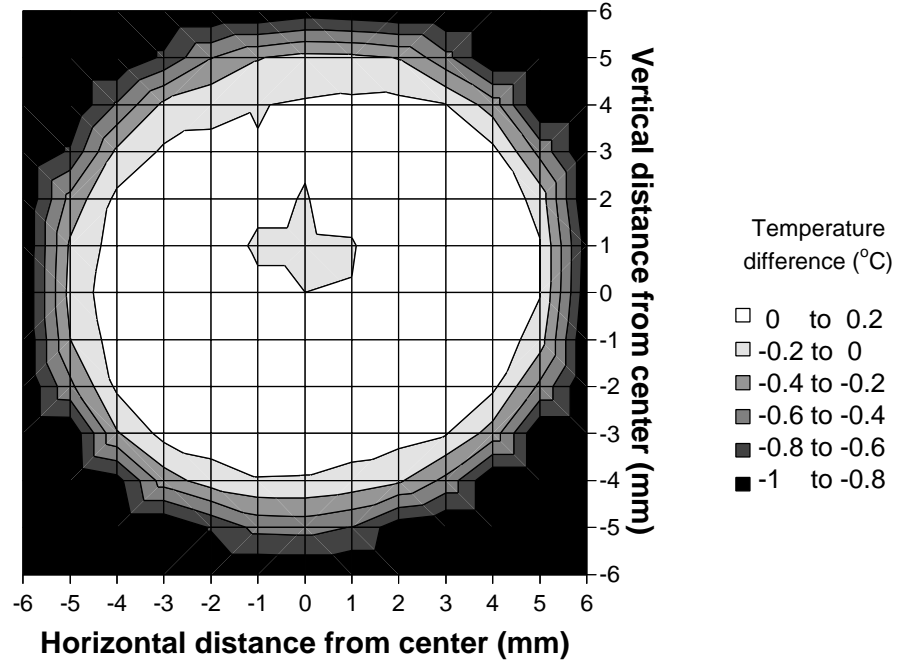


Figure 12. Spatial scan of the variable-temperature blackbody at 2000 °C. The temperature differences are from the center position (0,0).

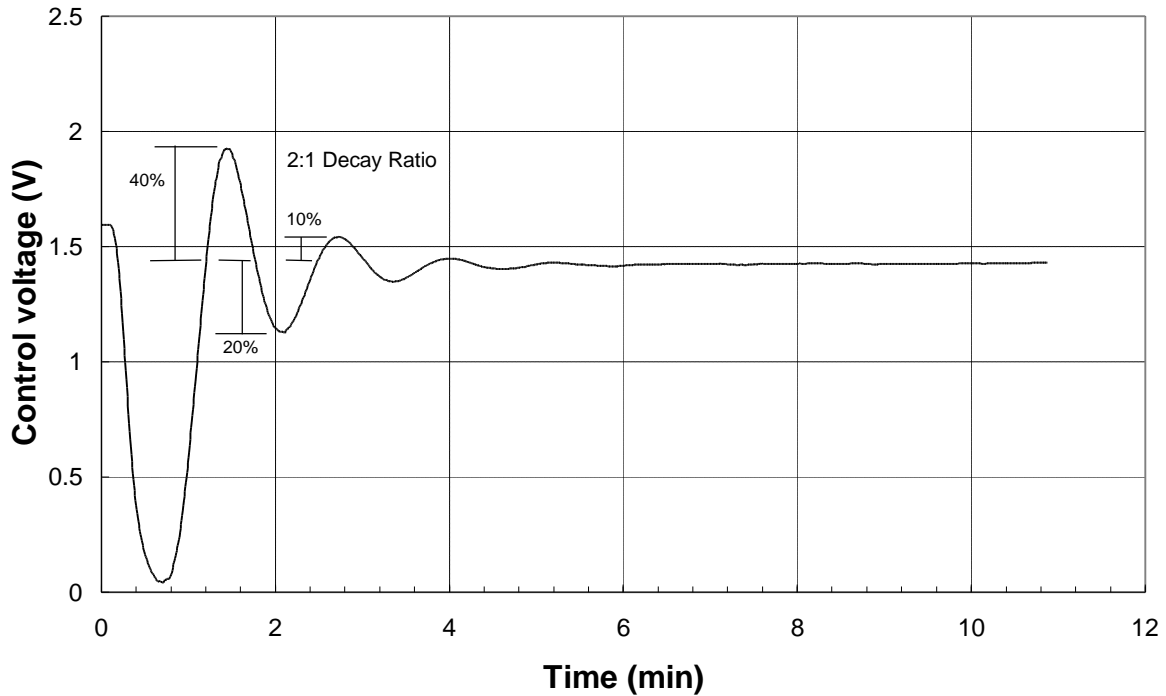


Figure 13. Variable temperature blackbody control. After decreasing the set point by 100 °C, the blackbody stabilizes in less than 10 min.

3.3 NIST photoelectric pyrometer

3.3.1 Measurement system

The PEP is a NIST designed transfer radiometer, which uses refractive optics to image the source onto the detector. The schematic of the NIST PEP is shown in figure 14. A drawing of the measurement system is shown in figure 15. The measurement system is completely automated and controlled by a personal computer, while the laboratory environment is monitored by temperature and relative humidity sensors. Lamps and blackbodies are positioned onto the optical axis of the PEP using a closed-loop motor controller system that allows positioning to within 0.01 mm. The components of the pyrometer are discussed in the next three sections followed by a discussion of the method used to characterize the system in the last three sections.

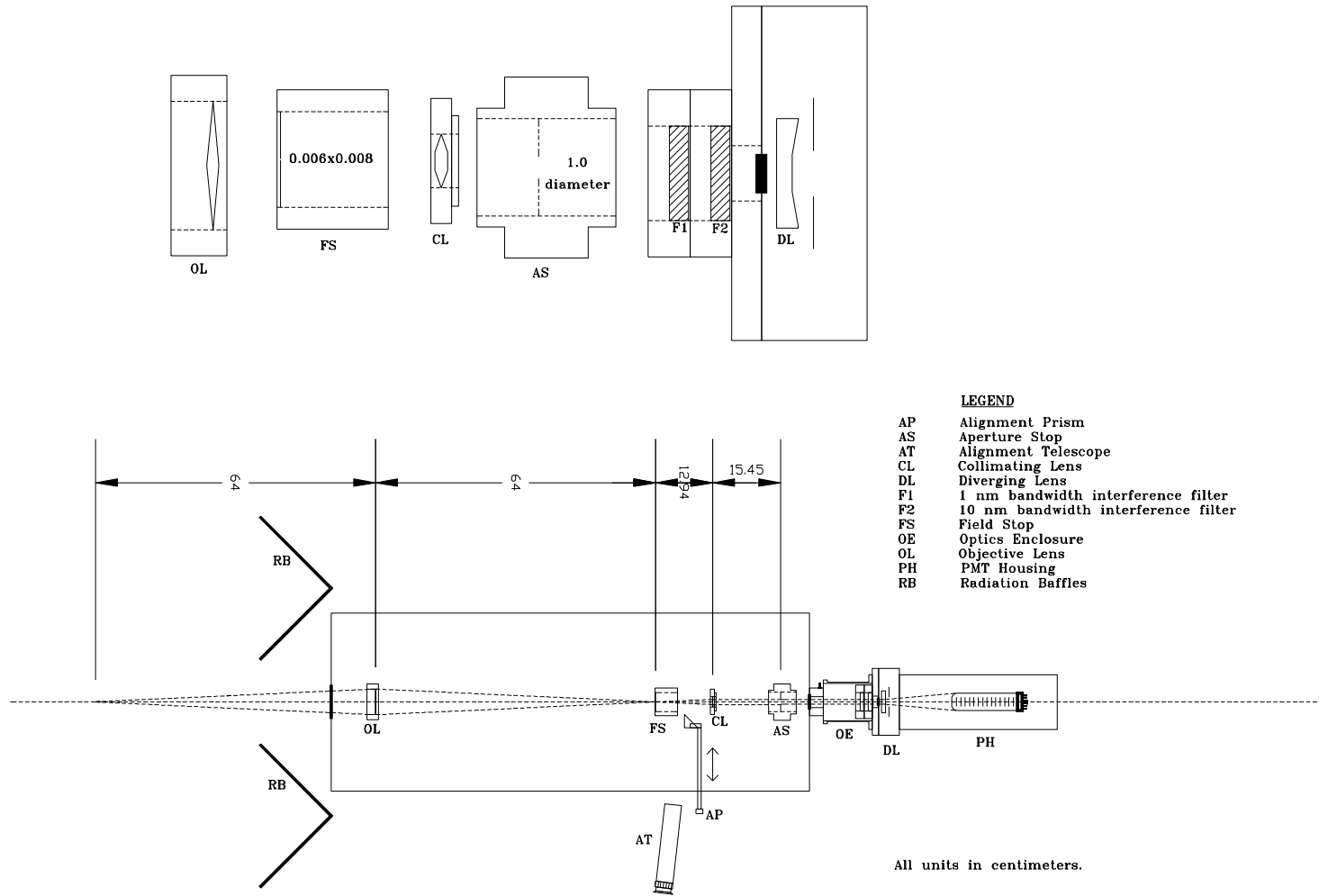
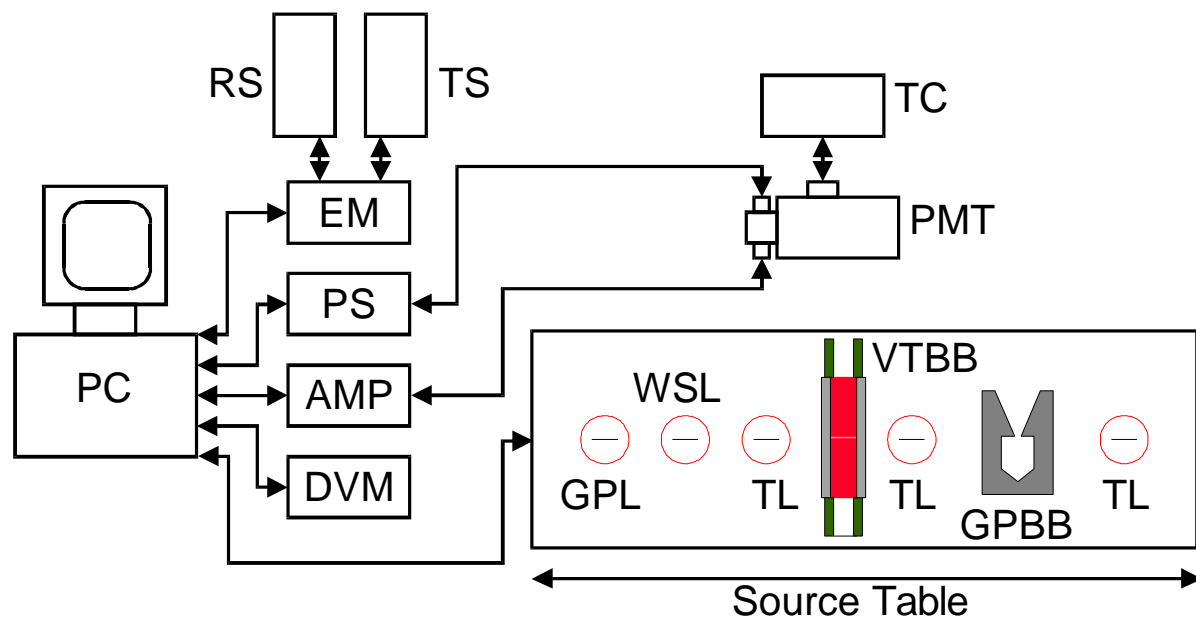


Figure 14. NIST photoelectric pyrometer.



LEGEND

AMP	Amplifier	PS	Power Supply
DVM	Digital Voltmeter	RS	Room Humidity Sensor
EM	Environmental Monitor	TC	Thermoelectric Cooler
GPBB	Gold-point Blackbody	TL	Test Lamp
GPL	Gold-point Lamp	TS	Temperature Sensor
PC	Personal Computer	VTBB	Variable Temperature Blackbody
PMT	Photomultiplier Tube	WSL	Working Standard Lamp

Figure 15. NIST radiance temperature laboratory measurement system.

3.3.2 Optical system

The first element is the objective lens (OL) which is a 5.8 cm diameter bi-convex lens with a focal length of 32 cm. The source is placed at twice the focal length from the lens and is imaged with unit magnification onto the field stop (FS), which is located at the back radius of curvature. The dimensions of the rectangular field stop are 0.6 mm wide by 0.8 mm high. The field stop defines the size and shape of the calibration target area. The next element is the collimating lens (CL), which is a 2.45 cm diameter bi-convex lens with a focal length of 12.94 cm. The field stop is placed at the front focal point of this lens with the result being a collimated beam with a diameter of approximately 1.2 cm. Next the aperture stop (AS) reduces the beam diameter to 1 cm. The beam continues through two interference filters (F1 & F2) through a plano-concave diverging lens that spreads the radiant flux over the photomultiplier tube cathode. The beam completely covers the surface of the cathode.

In all cases, the source overfills the objective lens and the aperture stop that corresponds to a system with an f -number of 13. The solid angle (4.67×10^{-3} sr) used is a cone having a half angle of 0.0772 rad (4.4°), the apex of which is at the center of the field stop.

To align sources, the field stop is removed, and the alignment prism (AP) is placed in the

path behind the field stop mount. The operator views the lamp filament or blackbody aperture and moves the filament or aperture to the target area viewed by the PEP.

3.3.3 Interference filters

The PEP uses two interference filters centered on 655.3 nm to produce a very narrow spectral bandwidth filter pack with transmittances in the wings six orders of magnitude lower than the peak. The first filter is a three-cavity type, and the second is a four-cavity type. Both are 5.08 cm diameter filters made from polished optical quality glass and are coated with a metal film. The regular spectral transmittances of the filters (see fig. 16) were measured from 400 nm to 1000 nm in 0.2 nm steps (with a relative expanded uncertainty of 0.3 % at 655 nm) using the NIST Transfer Spectrophotometer for Regular Transmittance described in reference [13]. The expanded uncertainty of the wavelength calibration of the spectrometer used to make these measurements was 0.5 nm at 655 nm. The first and second filters have spectral bandwidths of 1 nm and 10 nm, respectively. The central wavelength of the filters measured in series was determined to be 654.9 nm with a bandwidth of 2.4 nm when using transmittance data around the peak from 644 nm to 667 nm. For the full spectral range, the measured central wavelength was 836.6 nm with a bandwidth of 9.4 nm. The central wavelength I_c was determined from the following equation for determining the effective wavelength,

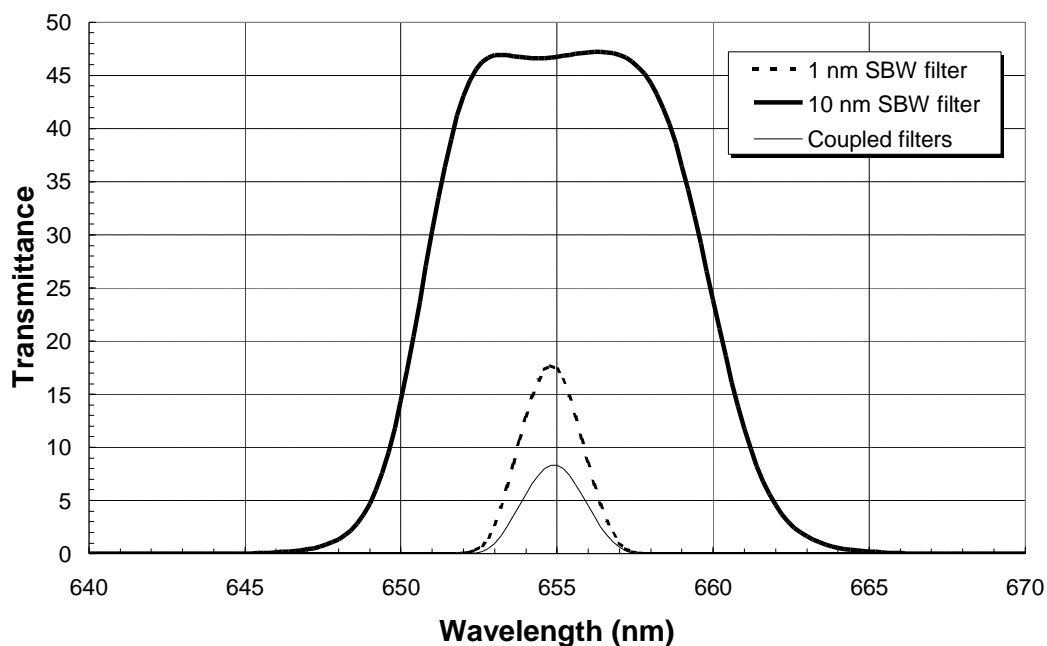


Figure 16. NIST photoelectric pyrometer filter transmittances. The wavelength of the pyrometer is selected by using a 1 nm and a 10 nm spectral bandwidth (SBW) filter.

$$I_c = \frac{\int I \cdot t_l \cdot dI}{\int I t_l \cdot dI} . \quad (17)$$

By approximating the integral with finite sums over equal wavelength bandwidths dI , I_c is found to be

$$I_c = \frac{\sum_{i=400}^{800} (I_i \cdot t_i)}{\sum_{i=400}^{800} t_i} , \quad (18)$$

where the value of i indicates the wavelength in nm. The spectral bandwidth ΔI_s was determined from the following integral relationship,

$$\Delta I_s = \frac{\int t_l \cdot dI}{t_{\text{peak}}} . \quad (19)$$

When the integral is converted into finite sums, the SBW becomes

$$\Delta I_s = \frac{\sum_{i=400}^{800} (t_i \cdot \Delta I_i)}{t_{\text{peak}}} . \quad (20)$$

3.3.4 Detectors

The PEP uses an 11-stage photomultiplier tube with a quartz window and an extended S-20 spectral response to measure spectral radiances. The detector is housed in a thermoelectrically cooled (-25 °C) chamber. The anode current is amplified and converted to a 0.1 V to 10 V signal by a programmable dc current amplifier and measured using a high accuracy digital voltmeter, capable of integration times ranging from 0.2 s to several minutes.

The signals for the test source and the WS lamp can vary by as much as a factor of 1100. Because several amplifier gain settings are required to cover this dynamic range, all signals are normalized to the 10^8 V/A range. The amplifier normalization factors C_A are determined by measuring the values of the four amplifier feedback resistors. Electrical currents I in the range from 1 nA to 1000 nA are supplied to the current amplifier, and the output voltages V are measured using a digital voltmeter. The resistances R , determined using Ohm's law, $V = I @R$, are R_7 , R_8 , R_9 , and R_{10} , for the (10^7 , 10^8 , 10^9 , and 10^{10}) V/A ranges, respectively. The normalization

factors for each range are shown in table 3.

Table 3. Current amplifier normalization factors

Range [V/A]	Normalization factor
10^7	$C_{A,R7} = R_8/R_7 = 9.9776$
10^8	$C_{A,R8} = R_8/R_8 = 1$
10^9	$C_{A,R9} = R_8/R_9 = 9.9858 \text{ H } 10^{-2}$
10^{10}	$C_{A,R10} = R_8/R_{10} = 9.9846 \text{ H } 10^{-3}$

3.3.5 Linearity of response

The degree of linearity of the PEP response is determined with a NIST designed automated beam conjoiner [14]. A beam from a constant source is split into two branches, whose fluxes are independently attenuated or blocked before recombination and further attenuation. The flux contribution from both branches is equal to the sum of the fluxes from each branch when measured separately (additivity). The device provides 100 levels of flux ranging over a factor of about 500. The levels are presented in random order to avoid systematic errors, and are interspersed with 25 zero flux levels. A personal computer controls the attenuating filters and records the filter positions and radiometer signals. The data is least-squares fitted to a polynomial response function to determine a correction factor (C_L) by which the radiometer output signal must be multiplied to obtain a quantity proportional to radiant flux. The correction factor is given by

$$C_L = \text{flux} / \text{signal} = (A_0 + A_1 \cdot S + A_2 \cdot S^2) / S, \quad (21)$$

where A_0 , A_1 , and A_2 are the coefficients found from the least squares approximation and S is the signal as defined in eq (1). The current values for the coefficients are listed in table 4. The magnitude of linearity correction factors is graphically shown in figure 17.

The measured instrument response is linear to within " 0.2 % for a range of photomultiplier anode currents from 0.1 nA to 500 nA. For currents much less than 0.1 nA, the signal is limited by noise. In order to ensure linearity of response, the current is restricted to a maximum of 500 nA by selection of the appropriate photomultiplier tube voltage. Typical default hardware settings used by the calibration program are listed in table 5.

Table 4. Detector system correction factors and linearity coefficients

Gain [V/A]	C_L	C_L	A_0 [V]	A_1	A_2 [V ⁻¹]
10^7	0.9987 for 500 nA	0.9973 for 1000 nA	$-2.1274 \text{ H } 10^{-8}$	1	$-2.6687 \text{ H } 10^{-4}$
10^8	0.9998 for 50 nA	0.9996 for 100 nA	$-2.1308 \text{ H } 10^{-6}$	1	$-3.8995 \text{ H } 10^{-5}$
10^9	1.0002 for 5 nA	1.0003 for 10 nA	$-8.9698 \text{ H } 10^{-9}$	1	$-3.1787 \text{ H } 10^{-5}$

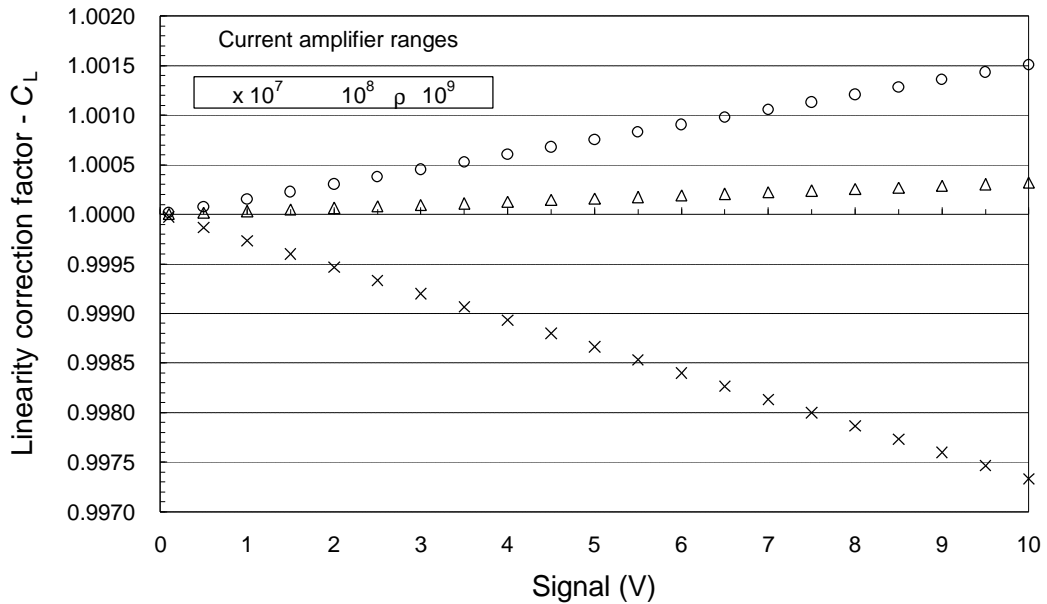


Figure 17. The linearity correction factors for the PEP.

Table 5. Default hardware settings used by calibration program

Temp [°C]	SL20 Signal [V]	Gain	Range Factor	SL20 Range Correction	L_I (SL20) [W·cm ⁻³ ·sr ⁻¹]	L_I (TEST) [W·cm ⁻³ ·sr ⁻¹]	Ratio Range Correction	Test Range Correction	Gain	Range Factor	Test Signal [V]	PMT HV [V]	Wait Time [min]
800	0.95	7	9.9776	9.4787	575.055	1.3015×10^0	2.2633×10^{-3}	0.0215	9	0.09986	0.2148	730	20
1100	0.95	7	9.9776	9.4787	575.055	1.1324×10^2	1.9693×10^{-1}	1.8666	8	1	1.8666	730	10
1500	1	9	0.099858	0.0999	575.055	4.1608×10^3	7.2355×10^0	0.7225	9	0.09986	7.2355	439	10
1900	1	9	0.099858	0.0999	575.055	4.0567×10^4	7.0544×10^0	7.0444	8	1	7.0444	439	5
2300	0.3	9	0.099858	0.0300	575.055	1.9487×10^5	3.3887×10^0	10.1517	7	9.9776	1.0174	385	5
3000	0.3	9	0.099858	0.0300	575.055	1.2079×10^6	2.1004×10^0	62.9232	7	9.9776	6.3064	385	5

3.3.6 Wavelength calibration

The mean effective wavelength of the PEP is calculated for temperature from 800 EC to 3000 EC by measuring its relative spectral response in the NIST Visible/Near Infrared Spectral Comparator Facility [15]. The collimating lens, aperture stop, optics enclosure, and PMT system of the PEP were set up in the Spectral Comparator Facility and the relative spectral response was measured while maintaining the same system geometry as in the RTCL. The PEP was measured from 400 nm to 900 nm in 5 nm steps and from 630 nm to 670 nm in 0.2 nm steps. The relative spectral response was calculated from the following equation,

$$R_{\text{PEP}}(\lambda) = \frac{S_{\text{PEP}}(\lambda)}{\frac{S_{\text{m1}}(\lambda)}{S_{\text{W}}(\lambda)} \cdot R_{\text{W}}(\lambda) \cdot \frac{G_{\text{W}}}{G_{\text{PEP}}}}, \quad (23)$$

where $R_{\text{PEP}}(\lambda)$ is the relative spectral response of the PEP in [A/W] as defined in eq (2), $S_{\text{PEP}}(\lambda)$ is the signal from the PEP in [V], $S_{\text{m1}}(\lambda)$ is the signal from the monitor detector simultaneous with $S_{\text{PEP}}(\lambda)$, $S_{\text{W}}(\lambda)$ is the signal from the detector working standard (DWS), $S_{\text{m2}}(\lambda)$ is the signal from the monitor detector simultaneous with $S_{\text{W}}(\lambda)$, $R_{\text{W}}(\lambda)$ is the absolute spectral response of the DWS, G_{W} is the calibrated amplifier gain for the DWS in [V/A], and G_{PEP} is the calibrated amplifier gain for the PEP. The PEP results are relative spectral responses because the measurement was performed in the overfill mode that resulted in a slightly different spot size. From eq (18), the CW was determined to be 655.0 nm and the SBW was calculated to be 5.0 nm from eq (20) for data over the 400 nm to 900 nm range. The CW was 655.3 nm with a SBW of 4.2 nm for the 630 nm to 670 nm data. Relative to the peak value, the measured relative spectral responsivity values decrease to about 10^{-4} at 5 nm from the central wavelength and to about 10^{-6} at 50 nm as illustrated in figure 18. Spectral radiance as defined in eq (4) is a function of a single wavelength, λ . However, the PEP has a finite bandwidth, and the PEP measures radiance as defined by an integral form of the Wien equation,

$$L = \int_{400}^{900} \frac{c_1}{\lambda^5 \cdot \exp(c_2 / (\lambda \cdot T))} \cdot R_{\lambda} \cdot d\lambda, \quad (24)$$

which could be used in the ITS-90 definition of eq (14). In the RTCL, the single wavelength $\lambda_{T_1-T_2}$ used in eq (4) is defined as follows,

$$\lambda_{T_1-T_2} = \frac{c_2}{\ln(L_2 / L_1)} \cdot \left(\frac{1}{T_1} - \frac{1}{T_2} \right), \quad (25)$$

where $I_{T_1-T_2}$ is the mean effective wavelength, L_1 is the radiance of the test lamp at temperature T_1 , and L_2 is the radiance of the WS at temperature T_2 .

All of the temperature measurements are performed for a mean effective wavelength of 655.3 nm, and these corrections are calculated for the VTBB with an emissivity of 0.99. The spectral radiance $L_l(\lambda, \epsilon_l, T)$ of the blackbody is defined by eq (5) to be a function of the wavelength, spectral emissivity, and the temperature, while the temperature $T(\lambda, L_l, \epsilon_l)$ is defined by eq (6) to be a function of the wavelength, spectral emissivity, and the spectral radiance. The following steps are performed to calculate the corrections at 900 nm for $T_0 = 1073$ K.

- ⇒ Calculate $L_0 = 1.2856 \text{ W}\cdot\text{cm}^{-3}\cdot\text{sr}^{-1}$, where $\lambda = 655.3 \text{ nm}$, $\epsilon_l = 1$, and $T = T_0$
- ⇒ Calculate $T_1 = 1073.53 \text{ K}$, where $\lambda = 655.3 \text{ nm}$, $\epsilon_l = 0.99$, and $L_l = L_0$
- ⇒ Calculate $L_1 = 68.31 \text{ W}\cdot\text{cm}^{-3}\cdot\text{sr}^{-1}$, where $\lambda = 900 \text{ nm}$, $\epsilon_l = 0.99$, and $T = T_1$
- ⇒ Calculate $T_2 = 1072.80 \text{ K}$, where $\lambda = 900 \text{ nm}$, $\epsilon_l = 1$, and $L_l = L_1$

The corrections $T_2 - T_0$ that are added to the radiance temperature at 655.3 nm to determine the radiance temperatures at 900 nm and 1000 nm are given in table 6. These corrections are equivalent to a spectral radiance correction of -0.27 % at 900 nm and -0.34 % at 1000 nm.

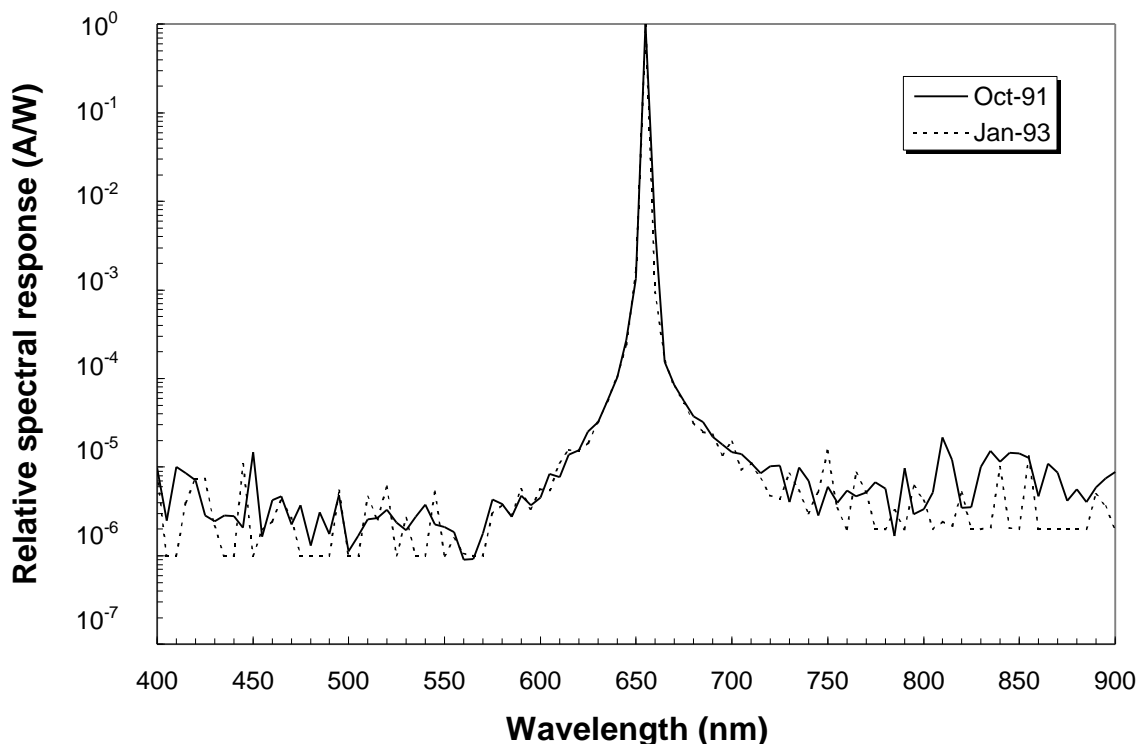


Figure 18. Relative spectral response of the NIST photoelectric pyrometer.

Table 6. Corrections ($^{\circ}\text{C}$) to the radiance temperature at 900 nm and at 1000 nm

Blackbody temperature ($^{\circ}\text{C}$)	900 nm	1000 nm
800	-0.20	-0.27
1100	-0.32	-0.45
1500	-0.53	-0.75
1900	-0.80	-1.13
2300	-1.12	-1.58
3000	-1.82	-2.55

3.3.7 Size of source effect

Measurements are performed to determine how much of the measured flux is from sources other than the target. This additional flux from outside the target area is scattered into the measured beam by the optical system. The measurement is performed to determine the size of source effect or the sensitivity of the PEP when viewing a 0.6 mm wide by 0.8 mm high target area on sources of various sizes. The magnitude of the size of source correction is determined by measuring the spectral radiance of a large uniform diffuse source with various apertures in front of the source. The large uniform diffuse source designed at NIST is used to measure the source of source effect. A 1 kW frosted quartz-halogen lamp is placed in a 20 cm by 23 cm by 20 cm vented housing. A lens focuses the lamp onto an opening in the housing that is covered by a diffuser. The apertures are on an aperture slide for quick positioning and reproducibility. The aperture sizes measured are a 1.4 mm by 25.4 mm slit, a 3 mm by 25.4 mm slit, a 15 mm diameter hole, and 25.4 mm diameter hole which approximate the sizes of the WS filament, the TL filament, the Au blackbody opening, and the BB opening. The ratio r_1 is the measurement of the ratio of the WS to the AuBB in eq (9). The size of source correction is calculated from the ratio of the measurements of the 15 mm diameter hole to the 1.4 mm by 25.4 mm slit. The spectral radiance correction was 0.09 %, which corresponds to a correction factor of 1.0009 ± 0.0006 and a temperature correction of 0.10°C . A negligible difference was observed for the comparison of the measurements of the 1.4 mm by 25.4 mm slit and the 3 mm by 25.4 mm slit; therefore, the correction factor for ratio r_2 is 1. The size of source correction for ratios r_3 and r_4 is -0.13% which corresponds to a correction factor of 0.9987 ± 0.0002 . The correction was calculated from the ratio of the measurements of the 1.4 mm by 25.4 mm slit to the 25.4 mm diameter hole. The magnitude of the temperature correction varies from -0.07°C at 800°C to -0.52°C at 2700°C . The size of source corrections are shown in figure 19. Because of flux contributions from outside the target area, the larger area BB results in a higher temperature. A negative correction is added to subtract the additional flux.

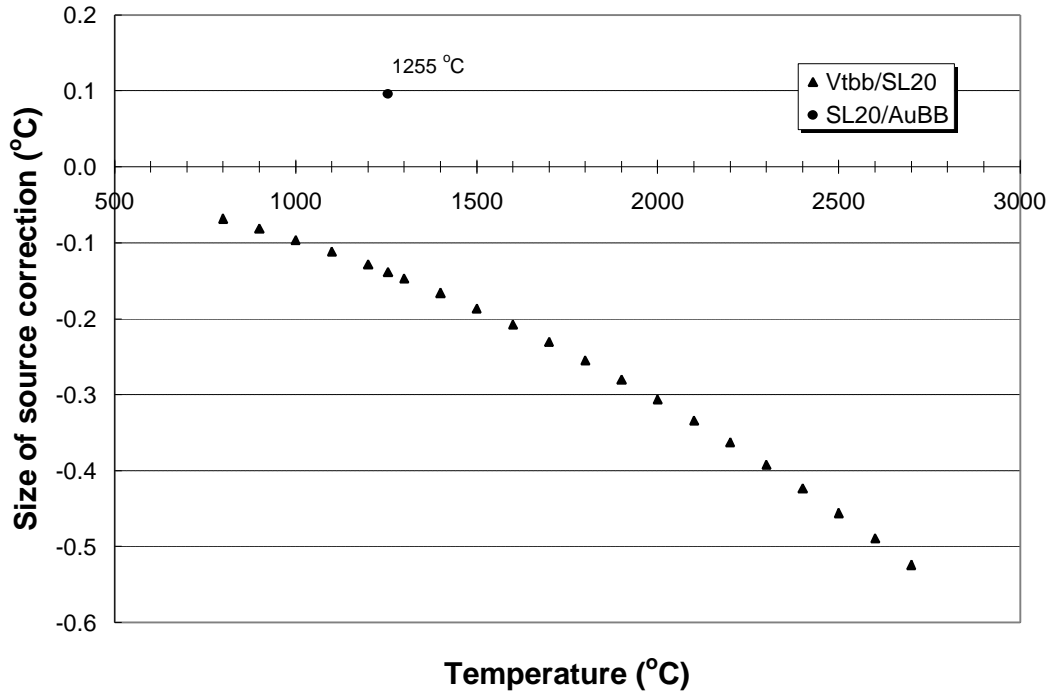


Figure 19. The size of source corrections for the variable temperature blackbody to the working standard lamp comparison and the working standard lamp to the gold-point blackbody.

3.4 Radiance temperature scale uncertainties

From the laws of statistical theory, when the covariances of the independent variables are assumed to be negligible, the propagation of standard uncertainty $u(y)$ for a variable y ,

$$y = f(x_1, x_2, x_3, \dots, x_N), \quad (26)$$

can be defined in terms of the following sum,

$$u(y) = \left[\sum_{i=1}^N \left(\frac{\partial f}{\partial x_i} \cdot u(x_i) \right)^2 \right]^{1/2}, \quad (27)$$

where $u(x_i)$ are the standard uncertainties. The uncertainty in the WS lamp spectral radiance,

$$\begin{aligned}
u_0(L_{\text{WS}}) = & \left[\left(\frac{\partial L_{\text{WS}}}{\partial n_1} \cdot u(n_1) \right)^2 + \left(\frac{\partial L_{\text{WS}}}{\partial I} \cdot u(I) \right)^2 + \left(\frac{\partial L_{\text{WS}}}{\partial T_{\text{Au}}} \cdot u(T_{\text{Au}}) \right)^2 \right. \\
& \left. + \left(\frac{\partial L_{\text{WS}}}{\partial c_2} \cdot u(c_2) \right)^2 + \sum_{i=1}^{11} \left(\frac{\partial L_{\text{WS}}}{\partial x_i} \cdot u(x_i) \right)^2 \right]^{1/2},
\end{aligned} \tag{28}$$

can be calculated by the root sum of squares (RSS) of the products of partial derivatives with their respective uncertainties. This uncertainty $u_0(L_{\text{WS}})$ can be derived directly from the measurement equation in eq (16) by using the propagation of standard uncertainty relationship in eq (27). The partial derivatives are those of the spectral radiance with respect to the independent variables in eq (16) and are listed in eqs (29) through (33). The eleven variables in the summation of eq (28) are the following variables: e_{Au} , c_{1L} , r_1 , $C_{\text{A,WS}}$, $C_{\text{L,WS}}$, $C_{\text{S,WS}}$, G_{WS} , $C_{\text{A,Au}}$, $C_{\text{L,Au}}$, $C_{\text{S,Au}}$, or G_{Au} . Since all of the measurements in the RTCL are based on the WS lamp, the uncertainty analysis of each calibration service (tungsten ribbon filament lamps, disappearing filament optical pyrometers, infrared thermometers) will be completed in Sections 4, 5, and 6 using the uncertainty in $u_0(L_{\text{WS}})$.

The measurement equation for the radiance temperature scale from the gold-point blackbody to the WS lamp can be represented by eq (16). The partial derivatives of the WS spectral radiance in eq (16) with respect to the variables, n_1 , I , T_{Au} , and c_2 , are

$$\frac{\partial L_{\text{WS}}}{\partial n_1} = \frac{L_{\text{WS}}}{n_1} \cdot \left[\frac{c_2}{n_1 \cdot I \cdot T_{\text{Au}}} \cdot \frac{\exp\left(\frac{c_2}{n_1 \cdot I \cdot T_{\text{Au}}}\right)}{\exp\left(\frac{c_2}{n_1 \cdot I \cdot T_{\text{Au}}}\right) - 1} - 2 \right], \tag{29}$$

$$\frac{\partial L_{\text{WS}}}{\partial I} = \frac{L_{\text{WS}}}{I} \cdot \left[\frac{c_2}{n_1 \cdot I \cdot T_{\text{Au}}} \cdot \frac{\exp\left(\frac{c_2}{n_1 \cdot I \cdot T_{\text{Au}}}\right)}{\exp\left(\frac{c_2}{n_1 \cdot I \cdot T_{\text{Au}}}\right) - 1} - 5 \right], \tag{30}$$

$$\frac{\partial L_{\text{WS}}}{\partial T_{\text{Au}}} = \frac{L_{\text{WS}}}{T_{\text{Au}}} \cdot \frac{c_2}{n_1 \cdot I \cdot T_{\text{Au}}} \cdot \frac{\exp\left(\frac{c_2}{n_1 \cdot I \cdot T_{\text{Au}}}\right)}{\exp\left(\frac{c_2}{n_1 \cdot I \cdot T_{\text{Au}}}\right) - 1}, \text{ and} \tag{31}$$

$$\frac{\partial L_{\text{WS}}}{\partial c_2} = \frac{-L_{\text{WS}}}{c_2} \cdot \frac{c_2}{n_1 \cdot I \cdot T_{\text{Au}}} \cdot \frac{\exp\left(\frac{c_2}{n_1 \cdot I \cdot T_{\text{Au}}}\right)}{\exp\left(\frac{c_2}{n_1 \cdot I \cdot T_{\text{Au}}}\right) - 1}. \quad (32)$$

The expression in eq (28),

$$\left| \frac{\partial L_{\text{WS}}}{\partial x} \right| = \frac{L_{\text{WS}}}{x}, \quad (33)$$

represents the partial derivatives of L_{WS} with respect to x , where x is one of the eleven variables in eq (28).

Table 7 details typical values of the variables in eq (16), while table 8 summarizes the uncertainties in eq (28). The uncertainty $u(T_{\text{Au}})$ in table 8 is derived from the NIST radiometric determination of the freezing point of gold [16]. The combined uncertainty $u(L_{\text{WS}})$ in the spectral radiance of the WS lamp can then be calculated by calculating the RSS from the following expression,

$$\frac{u(L_{\text{WS}})}{L_{\text{WS}}} = \left[\left(\frac{u_0(L_{\text{WS}})}{L_{\text{WS}}} \right)^2 + \left(\frac{u(\text{DMM})}{L_{\text{WS}}} \right)^2 + \left(\frac{u(\text{LTC})}{L_{\text{WS}}} \right)^2 + \left(\frac{u(\text{LD})}{L_{\text{WS}}} \right)^2 \right]^{1/2}, \quad (34)$$

where $u(\text{DMM})$ is the digital multimeter uncertainty, $u(\text{LTC})$ is the lamp current uncertainty, and $u(\text{LD})$ is the lamp drift uncertainty. From tables 7 and 8, a typical relative expanded uncertainty in the WS spectral radiance is equal to $(2.870 \text{ W}\cdot\text{m}^{-2}\cdot\mu\text{m}^{-1}\cdot\text{sr}^{-1})/(569.9 \text{ W}\cdot\text{m}^{-2}\cdot\mu\text{m}^{-1}\cdot\text{sr}^{-1})$, or 0.50 %. The final value of the WS spectral radiance will be utilized in Sections 4 through 6 to continue the uncertainty analyses for each type of calibration service.

3.5 Quality control

The Radiance Temperature Measurements Calibration Service ensures quality measurements through quality system implementation, internal quality control procedures, periodic audits, and interlaboratory comparisons. The Quality System Manual for the Radiance Temperature Measurements Calibration Service is based on the ANSI/NCSL Z540-1-1994 standard [17] and the ISO/IEC Guide 25 [18]. The Quality System Manual is organized into three sections that form a pyramidal shape. The top section is the Optical Technology Division Quality System Policies, the middle section contains the Division Procedures that uniformly apply to all the calibration services, and the bottom section is the Calibration Service Procedures for each calibration service. Additional information on the Divisions Quality System can be found in reference [19].

Table 7. Typical values of WS lamp variables and parameters

Variable	Symbol	Value
Refractive index	n_I	1.00028
Wavelength	I	655.3 nm
Freezing temperature of gold	T_{Au}	1337.33 K
Second radiation constant	c_2	14387.69 $\mu\text{m}\cdot\text{K}$
Emissivity of Au	e_{Au}	0.9999
First radiation constant	c_{1L}	$1.191 \times 10^8 \text{ W}\cdot\mu\text{m}^4\cdot\text{m}^{-2}$
Ratio of WS signal to Au signal	r_1	7.764
WS amplifier calibration correction	$C_{A,WS}$	1
WS linearity correction	$C_{L,WS}$	1
WS size of source correction	$C_{S,WS}$	1.0009
WS amplifier gain	G_{WS}	$1 \times 10^8 \text{ V}\cdot\text{A}^{-1}$
Au amplifier calibration correction	$C_{A,Au}$	1
Au linearity correction	$C_{L,Au}$	1
Au size of source correction	$C_{S,Au}$	1
Au amplifier gain	G_{Au}	$1 \times 10^8 \text{ V}\cdot\text{A}^{-1}$
WS spectral radiance	L_{WS}	$569.9 \text{ W}\cdot\text{m}^{-2}\cdot\mu\text{m}^{-1}\cdot\text{sr}^{-1}$

Table 8. Uncertainty budget for the NIST WS lamp spectral radiance realization

Uncertainty component	Symbol	Expanded Uncertainty ($k = 2$)	
		Type A	Type B
Refractive index	$u(n_1)$		0.00002
Wavelength	$u(\lambda)$		0.2 nm
Freezing temperature of gold	$u(T_{\text{Au}})$		0.23 K
Second radiation constant	$u(c_2)$		0.24 $\mu\text{m}\cdot\text{K}$
Emissivity of Au	$u(e_{\text{Au}})$		0.0002
First radiation constant	$u(c_{1L})$		440 $\text{W}\cdot\mu\text{m}^4\cdot\text{m}^{-2}$
Ratio of WS signal to Au signal	$u(r_1)$	0.006	
WS amplifier calibration correction	$u(C_{A,\text{WS}})$	0.0001	
WS linearity correction	$u(C_{L,\text{WS}})$	0.001	
WS size of source correction	$u(C_{S,\text{WS}})$	0.0006	
WS amplifier gain	$u(G_{\text{WS}})$		0 $\text{V}\cdot\text{A}^{-1}$
Au amplifier calibration correction	$u(C_{A,\text{Au}})$	0.0001	
Au linearity correction	$u(C_{L,\text{Au}})$	0.001	
Au size of source correction	$u(C_{S,\text{Au}})$	0.0002	
Au amplifier gain	$u(G_{\text{Au}})$		0 $\text{V}\cdot\text{A}^{-1}$
WS lamp spectral radiance	$u_0(L_{\text{WS}})$		2.754 $\text{W}\cdot\text{m}^{-2}\cdot\mu\text{m}^{-1}\cdot\text{sr}^{-1}$
Digital voltmeter	$u(\text{DMM})$		0.000 $\text{W}\cdot\text{m}^{-2}\cdot\mu\text{m}^{-1}\cdot\text{sr}^{-1}$
WS current	$u(\text{LTC})$		0.570 $\text{W}\cdot\text{m}^{-2}\cdot\mu\text{m}^{-1}\cdot\text{sr}^{-1}$
WS drift	$u(\text{LD})$	0.570 $\text{W}/\text{m}^2/\mu\text{m}/\text{sr}$	
NIST WS lamp spectral radiance	$u(L_{\text{WS}})$	2.870 $\text{W}\cdot\text{m}^{-2}\cdot\mu\text{m}^{-1}\cdot\text{sr}^{-1}$	
NIST WS lamp temperature	$u(T_{\text{WS}})$	0.536 K	

The calibrations resulting from the processes described in this document are derived in principle from a complete realization of the radiance temperature scale, and therefore are not dependent upon the maintenance of in-house standards. In practice, the realization often omits the GPBB comparison and relies upon the spectral radiance that is maintained on the stable working standard lamp. The calibration history of the lamp compared to the GPBB is monitored to confirm the stability of the lamp (see fig. 9). The working standard lamp is compared to the gold point blackbody at least twice a year. Lamp and radiation thermometer check standards are periodically measured to ensure the accuracy of the measurements. The calibration history of the ribbon filament lamp check standards (Serial numbers P51 and P74) are shown in figure 20, while the calibration history of the radiation thermometer check standard (Minolta Cyclops 52) is shown in figure 21. The calibration process is further monitored by using control limits in the data acquisition and data reduction programs. A check-list is used to track the status of the test unit throughout the calibration process. A calibration summary sheet is created for each calibrated item to record customer information, measurements performed, test unit information, environmental conditions, filenames, and computer programs used for data acquisition and reduction. The calibration report is carefully reviewed by a party who was not involved in producing the values.

Audits are performed annually by the Division's quality control team. This calibration service participates in bilateral and multilateral laboratory comparisons of radiance temperature with various national laboratories usually involving guest scientists [20,21].

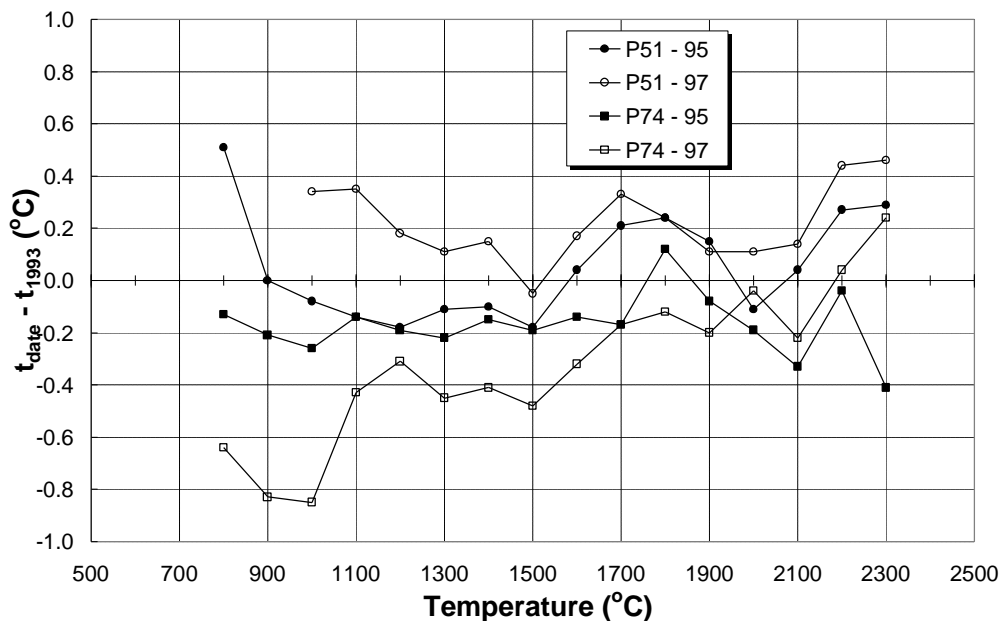


Figure 20. Calibration history of the ribbon filament lamp check standards.

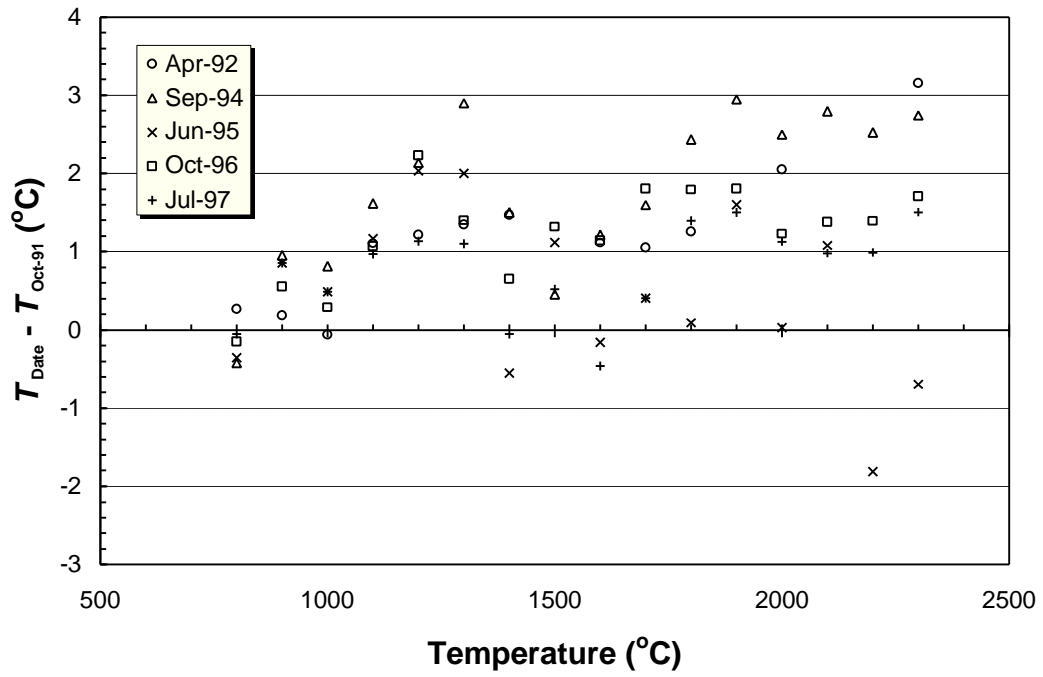


Figure 21. Calibration history of the radiation thermometer check standard (Minolta Cyclops 52).